CPUE standardization of blue marlin (*Makaira nigricans*) for the Taiwanese distant-water tuna longline fishery in the Pacific Ocean during 1971 - 2024

Zi-Wei Yeh and Yi-Jay Chang

Institute of Oceanography, National Taiwan University

Abstract

Pacific blue marlin (*Makaira nigricans*) is a highly migratory pelagic species widely distributed across the Pacific Ocean and is considered to form a single Pacific-wide stock. This study updates standardized catch-per-unit-effort (CPUE) indices for Pacific blue marlin from the Taiwanese distant-water tuna longline (DWLL) fishery for the period 1971 – 2024, in support of the forthcoming blue marlin stock assessment. Operational logbook data were analyzed using a spatio-temporal delta-lognormal generalized linear mixed modeling framework implemented in the *sdmTMB* package. To account for temporal changes in data availability, fishing practices, and fleet behavior, CPUE standardization was conducted separately for three periods: 1971 – 1978, 1979 – 1999, and 2000 – 2024. The models incorporated spatial and spatio-temporal random effects, vessel effects, and period-specific catchability covariates, including total hook numbers and hooks per basket (HPB). Model diagnostics based on probability integral transform residuals indicated satisfactory model performance with no strong spatial or temporal misfit. The resulting standardized indices show high interannual variability and large uncertainty during the early period, an overall declining trend during 1979 – 1999, and a relatively stable pattern with interannual variability during 2000 – 2023. Notably, the relative abundance index in 2024 increased sharply, reaching the highest level observed in the time series.

1. Introduction

Pacific blue marlin (*Makaira nigricans*) is a highly migratory species distributed throughout tropical and temperate waters of the Pacific Ocean. Evidence from genetic analyses (Graves and McDowell, 2003), fishery-dependent catch rate data (Kleiber *et al*., 2003), and tagging studies (Hinton, 2001) supports the existence of a single Pacific-wide stock. The Taiwanese distant-water tuna longline (DWLL) fishery has operated across the Pacific for more than five decades and provides important catch and effort information for blue marlin. In support of the next ISC stock assessment planned for 2026, this working paper updates the standardized catch-per-unit-effort (CPUE) indices for the Taiwanese DWLL fishery from 1971 to 2024. The CPUE standardization was conducted using a spatio-temporal delta-lognormal mixed modelling framework implemented in *sdmTMB* (Anderson *et al*., 2022), which explicitly accounts for spatial and spatio-temporal random effects in CPUE observations. The resulting standardized CPUE indices are intended to provide reliable relative abundance information for use in the forthcoming ISC assessment of Pacific blue marlin.

2. Materials and methods

2.1 Fishery data

Operational logbook data from the Taiwanese DWLL fleet in the Pacific Ocean during 1964 - 2024 were obtained from the Overseas Fisheries Development Council (OFDC). These data include catch number, hooks, fishing date (year, month), and fishing location recorded on a 1° × 1° grid, along with operational characteristics such as hooks per basket (HPB). Information on HPB is available beginning in 1995. Catch-per-unit-effort (CPUE) was calculated as the number of blue marlin caught per 1,000 hooks. Due to temporal changes in data quality, reporting formats, and fleet targeting behavior, the CPUE standardization was conducted separately for three periods: 1971 - 1978 (early), 1979 - 1999 (middle), and 2000 - 2024 (recent) (Hsu and Chang, 2020).

2.2 CPUE standardization model

The CPUE standardization was conducted using the *sdmTMB* package (https://github.com/pbs-assess/sdmTMB), a spatio-temporal modelling framework developed by Anderson *et al*. (2022). The model incorporates spatial correlation and spatio-temporal autocorrelation by estimating Gaussian random fields with a Matérn covariance structure. Spatial knots for each period were used as basis locations for estimating the spatial and spatio-temporal random effects. A delta-generalized linear mixed model (delta-GLMM) structure was applied, in which the probability distribution of CPUE is decomposed into two components:

(1) encounter rate component (binominal distribution):

$$\text{logit}(p) = \beta_1(t) + \omega_1(s) + \varepsilon_1(s,t) + \delta_1(v) + Q(k_1)$$

(2) positive catch rate component (lognormal distribution):

$$\log(q) = \beta_2(t) + \omega_2(s) + \varepsilon_2(s,t) + \delta_2(v) + Q(k_2)$$

where $\beta(t)$ is the temporal effect for t year as a fixed effect, $\omega(s)$ is the spatial random effect for knot s, $\varepsilon(s,t)$ is the spatio-temporal random effect for knot s in t year, $\delta(v)$ is the random effect variation in catchability for vessel *v*. $Q(k)$ is the fixed effect for k catchability covariate (i.e., total hook numbers and HPB for middle [1979 - 1999] and recent period [2000 - 2024], respectively). The choice of catchability covariates differed between periods based on data exploratory analysis. For the middle period (1979 - 1999), the total number of hooks was included as a covariate because it exhibited substantial inter-annual variability and a clear increasing trend over time, potentially influencing the effective fishing effort. For the recent period (2000 - 2024), HPB was incorporated as a factor to account for changes in vertical fishing strategy, as detailed set-level HPB records only became consistently available starting in 2000. Specifically, the effects of total hook numbers and HPB were modeled using smoothing splines with a default basis dimension, allowing for non-linear relationships with catch rates. Residual diagnostics

were conducted using probability integral transform (PIT) residuals, evaluated with the *DHARMa* R package (Hartig and Lohse, 2017).

2.3 Estimated abundance indices

Estimated values of fixed and random effect are used to predict the density, $d(s,t)$, for knot s and year t except for the catchability variables:

$$d(s,t) = \text{logit}^{-1}(\beta_1(t) + \omega_1(s) + \varepsilon_1(s,t)) \times \exp(\beta_2(t) + \omega_2(s) + \varepsilon_2(s,t))$$

When predicting the annual abundance indices, the catchability covariates were kept constant to standardize the effort. Specifically, the total hook numbers in the middle-period model and HPB in the recent-period model were fixed at their respective grand means across the entire study period. Then, the yearly index of abundance of blue marlin, $I(t)$, is calculated as the sum of the density of each knot by using an area-weighted approach:

$$I(t) = \sum_{s=1}^{n_s} A(s) \times d(s,t)$$

where $I(t)$ is the area re-weighted density in year t throughout the population domain, $a(s)$ is the area of knot s.

3. Results

3.1 Spatio-temporal distribution of fishery data

In this study, we compiled publicly available 5° × 5° latitude-longitude data from the WCPFC and IATTC to summarize historical annual catches by national fleets from 1950 - 2023. As shown in **Figure 1**, the major fishing nations, in descending order of total catch, were Japan, Taiwan, Korea, China, and the United States. The spatiotemporal distribution and annual species composition of TWN DWLL during 1971 - 2024 are shown in **Figures 2** and **3**. Since 2000, tropical tuna fisheries have become increasingly dominant, with the proportions of yellowfin tuna and bigeye tuna catches rising markedly. In addition, the spatiotemporal distributions of nominal CPUE and mean body weight (total catch divided by number of individuals) of blue marlin in the Taiwanese DWLL fishery are shown in **Figures 4** and **5**. Blue marlin exhibit higher catch rates in tropical regions, while fishing activity in temperate areas of the North Pacific began to emerge around 1995. Prior to 2000, effort in the North Pacific was limited, resulting in only patchy observations. After 2000, blue marlin in tropical regions east of 150°W tended to show relatively higher mean body weights. It is noted that the catch rates in tropical waters in 2024 were higher than in previous years, with particularly pronounced increases in areas west of 180° longitude.

3.2 Model diagnostics

Figure 6 shows PIT residuals aggregated across years at each spatial grid for the three period-specific models. The PIT residual distributions are approximately uniform, suggesting adequate model fit for each period (**Figure 6a**). Also, spatial PIT values are generally centered around 0.5, with no clear large-scale spatial structure, indicating no obvious spatially systematic model misfit for each period (**Figure 6b**).

3.3 Derived relative abundance indices for blue marlin

For the 1979 - 1999 period, **Figure 7a** shows a gradual shift toward higher total hook numbers, while **Figure 7b** indicates that increasing hook numbers are associated with higher encounter probability but lower catch rates in the standardized model. Additionally, in the 2000 - 2024 period, **Figure 8a** shows an increasing prevalence of higher HPB configurations, while **Figure 8b** indicates that higher HPB is associated with reduced encounter probability and lower catch rates in the standardized model.

The derived relative abundance indices, together with the spatial distributions of observed CPUE and knot mesh used in the standardized model, for blue marlin across three periods were shown in **Figure 9**. Specifically, during the early period (1971 - 1978), interannual variability was high and uncertainty was relatively large. Most CPUE observations (98% of data) were concentrated in the South Pacific, and consequently, the estimated relative abundance index during this period mainly reflects conditions in the South Pacific. In the middle period (1979 - 1999), the relative abundance showed an overall declining trend, with an increase in 1994. Similar to the early period, CPUE observations remained largely concentrated in the South Pacific (95% of data), and abundance estimates were therefore still dominated by this region. In contrast, the estimated relative abundance in the late period (2000 - 2024) exhibited fluctuated pattern. CPUE observations increased notably in the North Pacific, resulting in abundance estimates that reflect a broader basin-wide distribution. Notably, relative abundance in 2024 increased sharply, reaching the highest level observed in the time series.

References

Anderson, S. C., Ward, E. J., English, P. A., and Barnett, L. A. K. (2022). sdmTMB: an R package for fast, flexible, and user-friendly generalized linear mixed effects models with spatial and spatiotemporal random fields. preprint, Ecology.

Graves, J.E., McDowell, J.R. (2003). Stock structure of the world's istiophorid billfishes: a genetic perspective. Mar. Freshw. Res., 54: 287 - 298.

Hartig, F. and Lohse, L. (2017). Residual diagnostics for hierarchical (multi-level/mixed) regression models. R package version 0.1, 5:1 - 21.

Hinton, M.G. (2001). Status of blue marlin in the Pacific Ocean. Inter-American Tropical Tuna Commission (IATTC), Stock Assessment Report 1, pp. 284 - 319.

Hsu, J., and Chang, Y. J. (2020). CPUE standardization of blue marlin (*Makaira nigricans*) for the Taiwanese distant-water tuna longline fishery in the Pacific Ocean during 1971 - 2019. ISC/20/BILLWG-03/03.

Kleiber, P., Hinton, M.G., Uozumi, Y. (2003). Stock assessment of blue marlin (*Makaira nigricans)* in the Pacific using MUNTIFAN-CL. Mar. Freshw. Res., 54: 349 - 360.

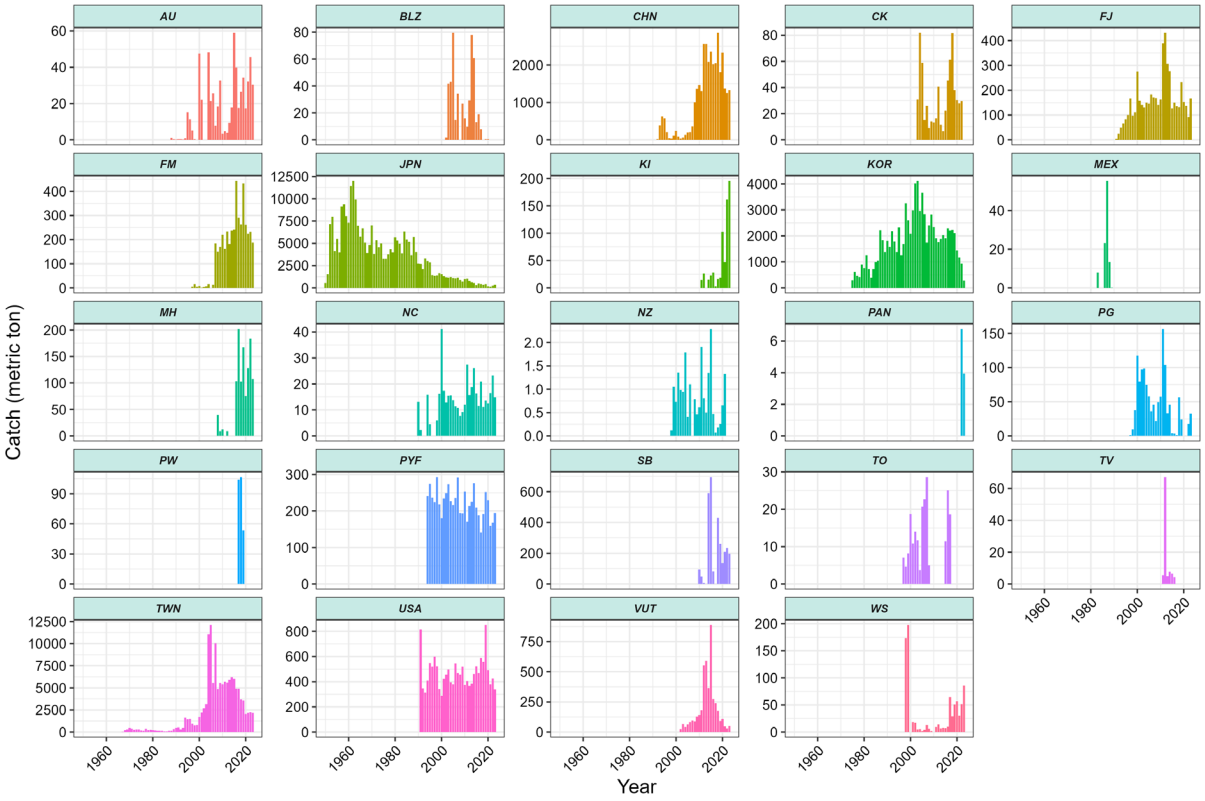

Figure 1. Annual catch (in metric tons) of Pacific blue marlin by national longline fleets, derived from publicly available datasets of the WCPFC and IATTC during 1950 - 2024.

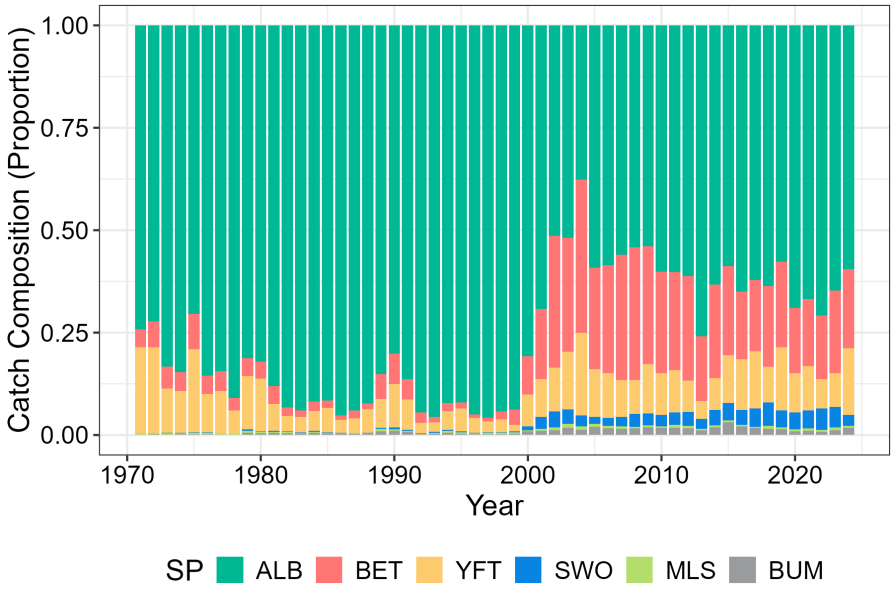

Figure 2. Annual species composition (proportional catch) of the Taiwanese distant-water longline (TWN DWLL) fishery in the Pacific Ocean during 1971 - 2024. ALB = albacore, BET = bigeye tuna, YFT = yellowfin tuna, SWO = swordfish, MLS = striped marlin, and BUM = blue marlin.

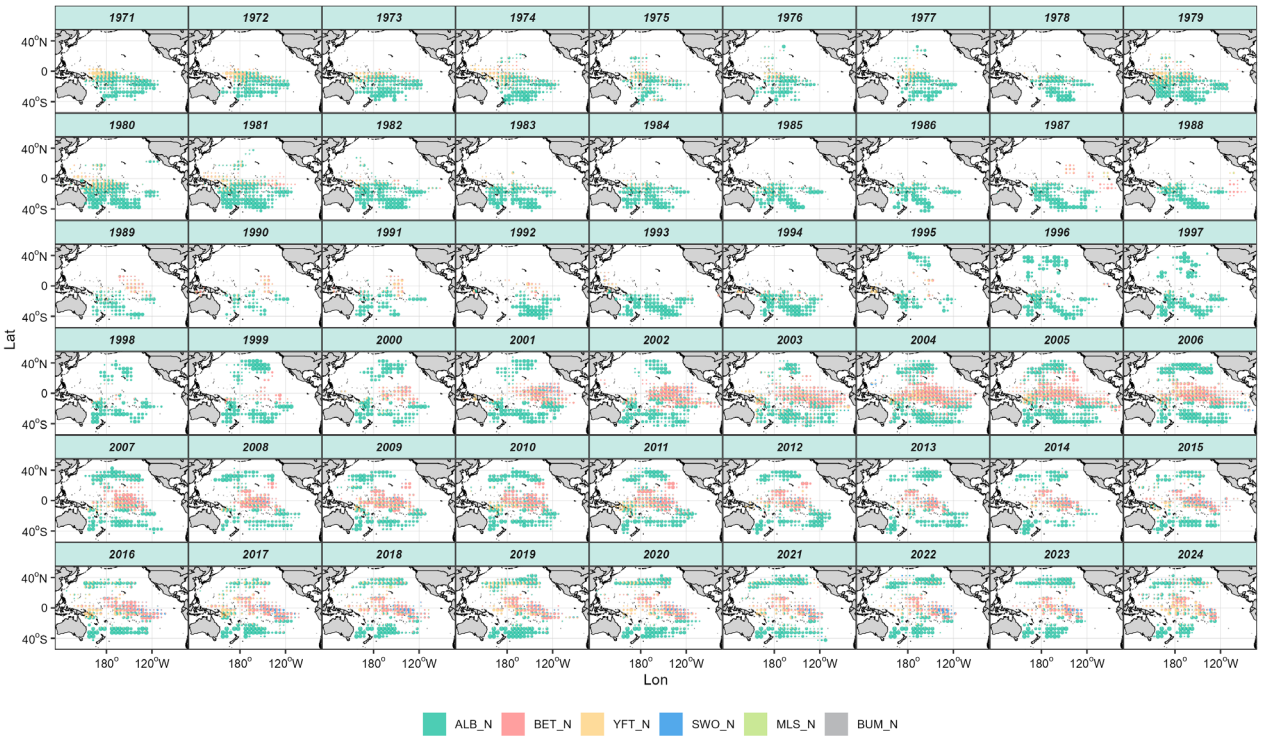

Figure 3. Spatial distributions of species composition (proportional catch) for the Taiwanese distant-water longline (TWN DWLL) fishery in the Pacific Ocean during 1971 - 2024. Operational data were aggregated into 5 × 5 grids per year. The colors represent the proportion of different species, and the circle sizes reflect the relative catch in number.

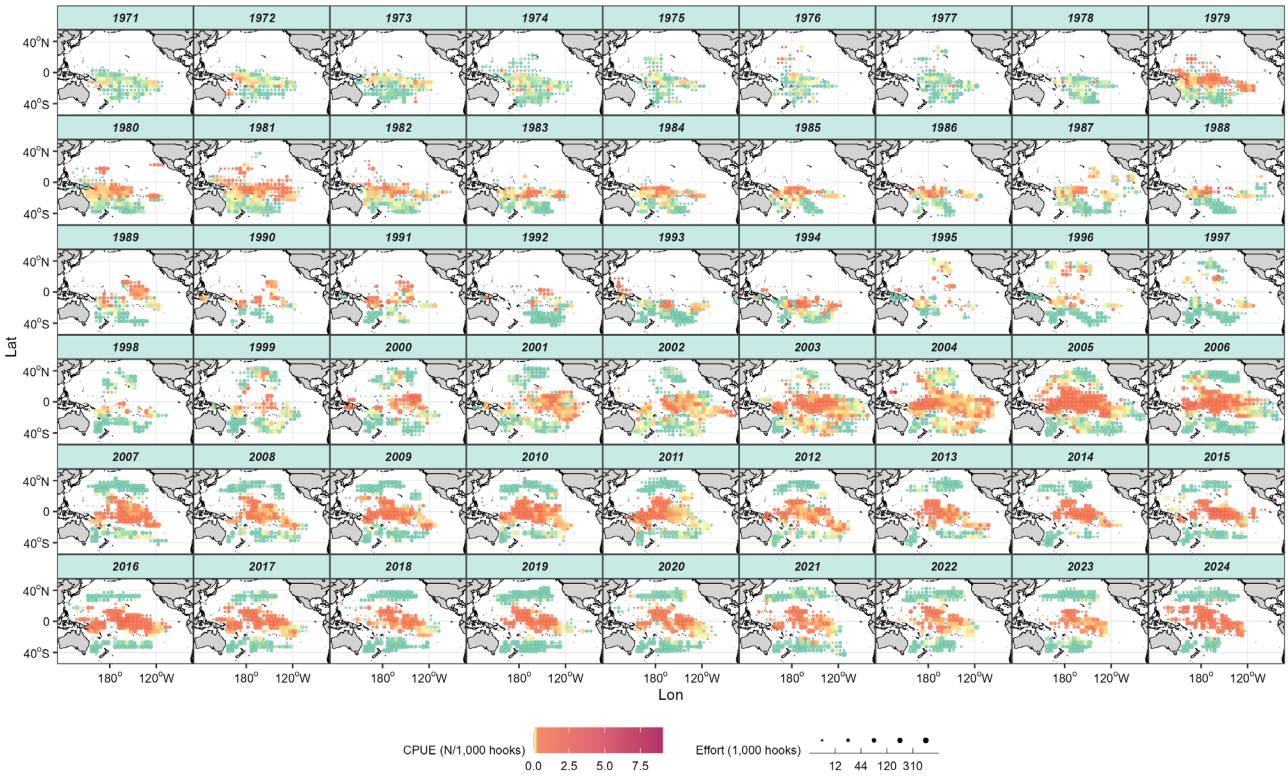

Figure 4. Spatial distributions of observed CPUE (N/1,000 hooks) and fishing efforts (in 1,000 hooks) for blue marlin in the Taiwanese distant-water longline (DWLL) fishery across the Pacific Ocean during 1971 - 2024. Circle size indicates fishing effort within each spatial grid. The nominal CPUE was calculated at a 5 × 5 grid resolution per year by dividing the total catch in number by the total fishing effort (1,000 hooks). Circle size indicates the fishing effort within each spatial grid.

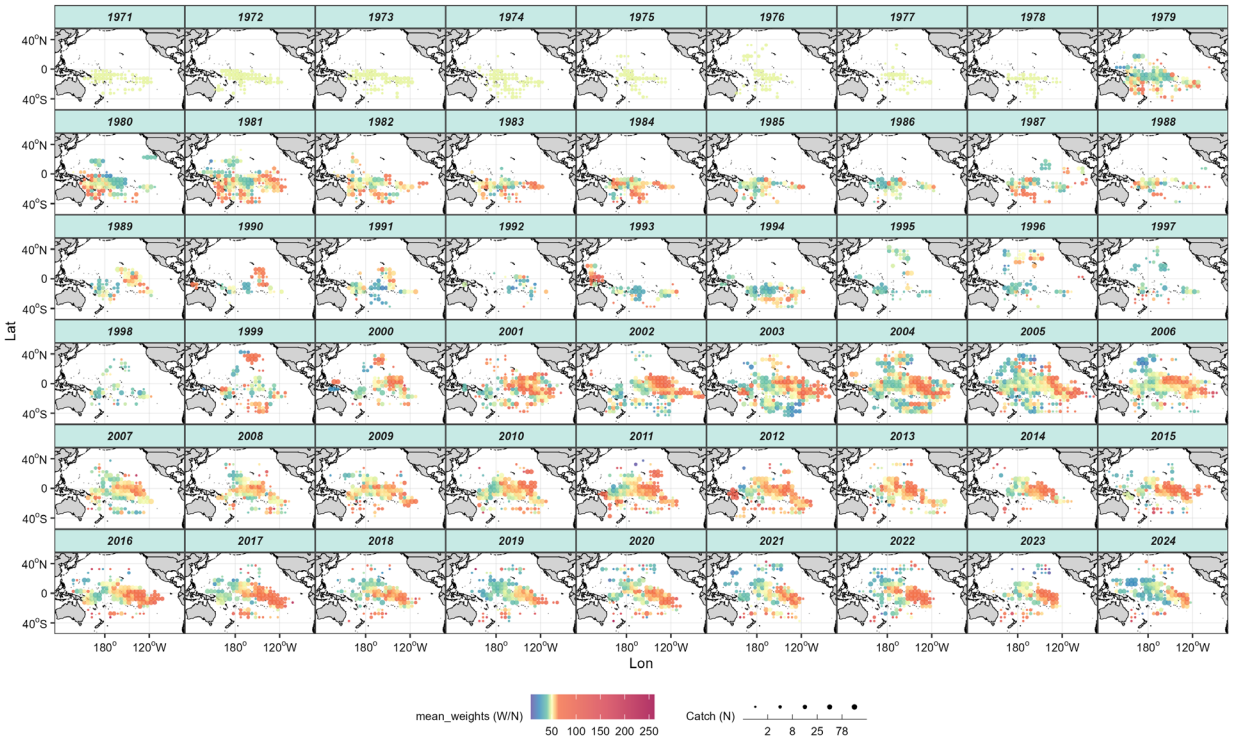

Figure 5. Spatial distribution of average weight (total catch divided by number of individuals) of blue marlin in the Taiwanese distant-water longline (DWLL) fishery in the Pacific Ocean from 1971 to 2024. Circle size indicates the total catch (in number) of blue marlin within each spatial grid. The average weight was calculated at a 5 × 5 grid resolution per year by dividing the total catch in weight by the total catch in number. Circle size indicates the total catch in number of blue marlin within each spatial grid.

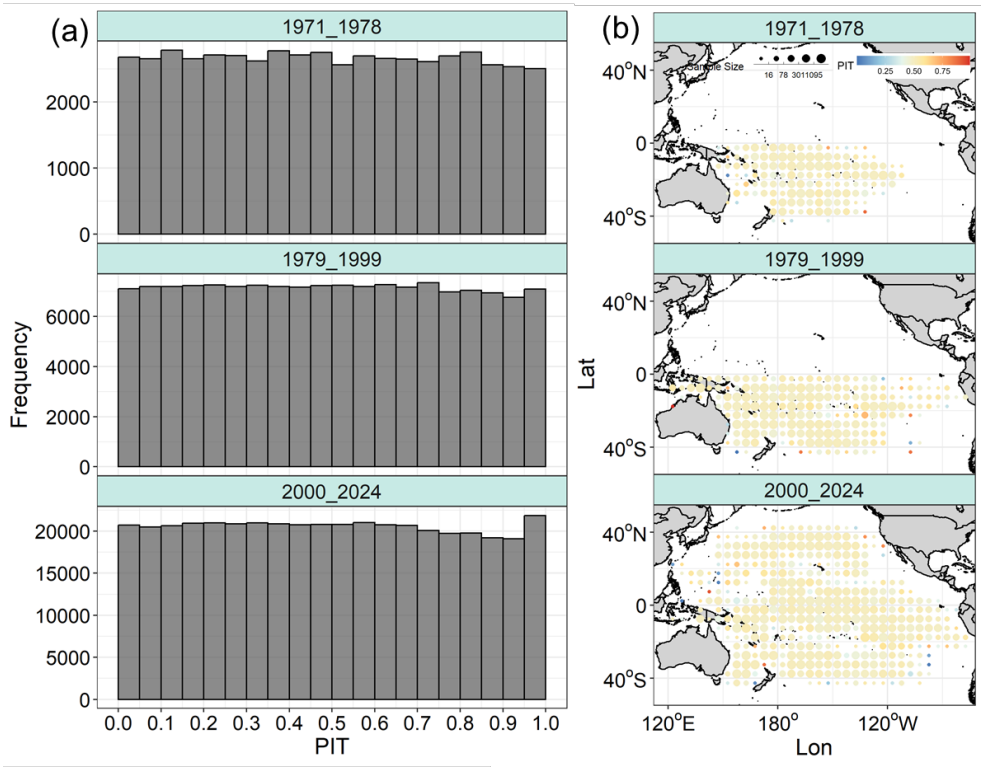

Figure 6. Probability Integral Transform (PIT) diagnostics for period-specific *sdmTMB* models fitted to blue marlin data from the Taiwanese distant-water longline (TWN DWLL) fishery. (a) Distributions of PIT residuals for the three fitted periods (1971 - 1978, 1979 - 1999, and 2000 - 2024). (b) Spatial distributions of the mean PIT residuals for each period-specific model, calculated by averaging residuals within each spatial grid.

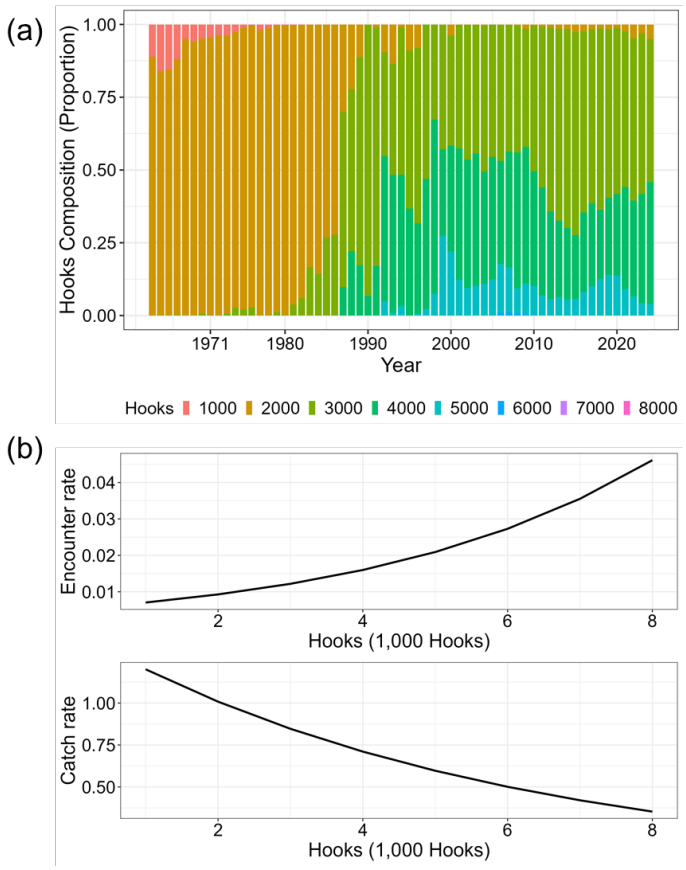

Figure 7. Annual composition and modeled effects of total hook numbers in the Taiwanese distant-water longline (DWLL) fishery during 1979 - 1999. (a) temporal changes in the proportional composition of total hook numbers. (b) Estimated effects of total hook numbers on encounter probability and catch rate from the standardized model.

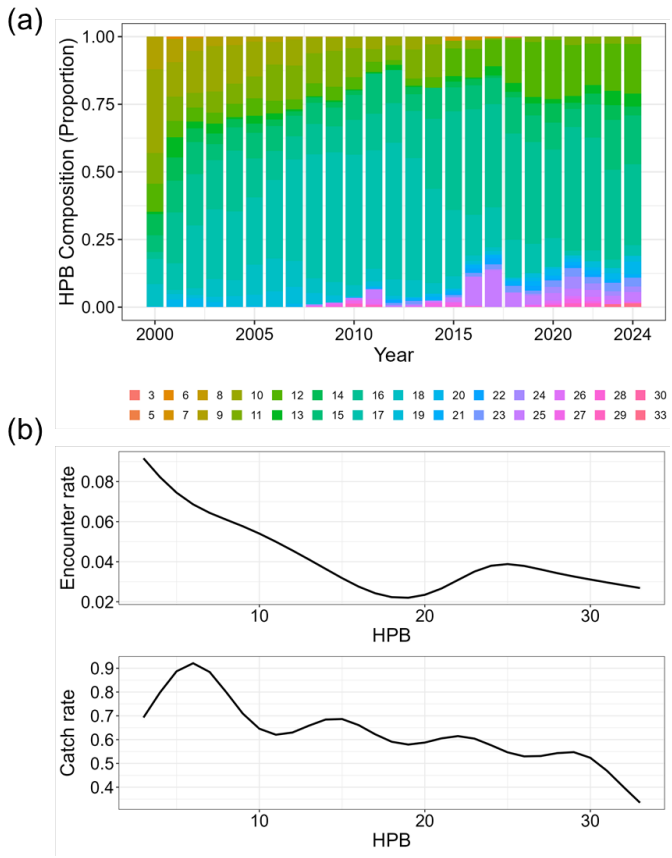

Figure 8. Annual composition and modelled effects of hooks per basket (HPB) in the Taiwanese distant-water longline (DWLL) fishery during 2000 - 2024. (a) Temporal changes in the proportional composition of HPB. (b) Estimated effects of HPB on encounter probability and catch rate from the standardized model.

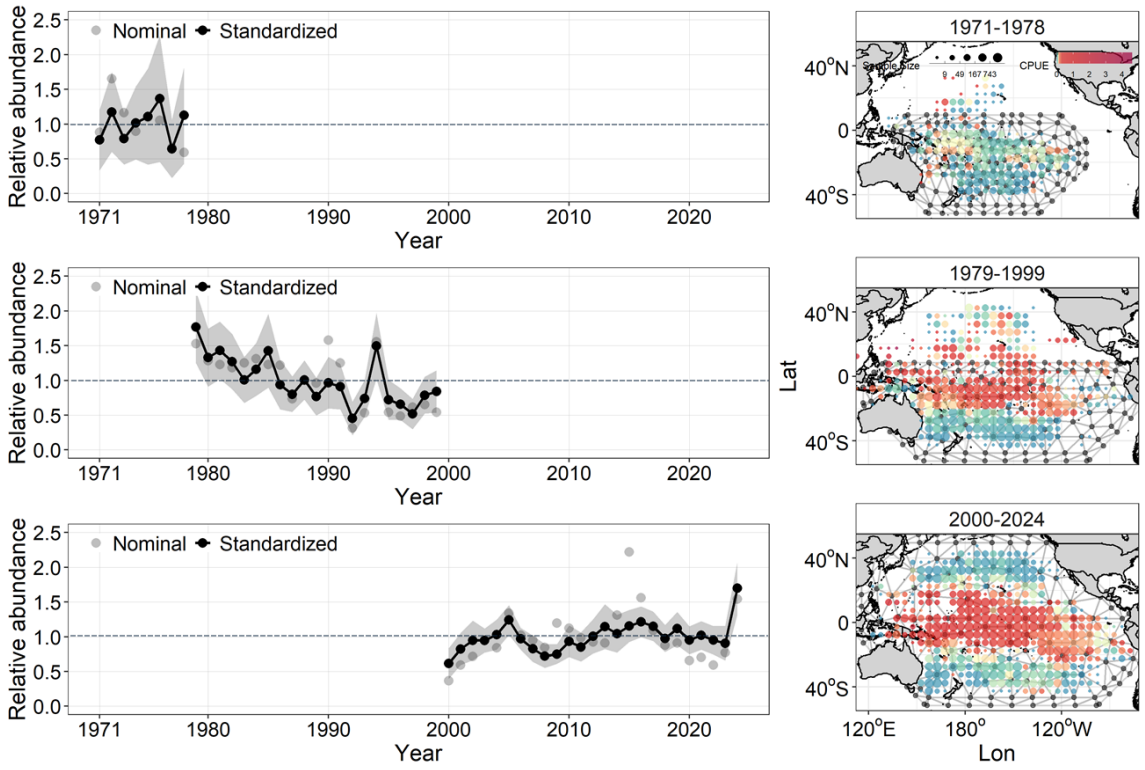

Figure 9. Period-specific relative abundance indices of blue marlin estimated using *sdmTMB* from Taiwanese distant-water longline (DWLL) fishery data for 1971 - 1978, 1979 - 1999, and 2000 - 2024. Left panels show nominal and standardized indices, while right panels display the spatial knot meshes used in each model.